Large-amplitude vibrations of doubly-curved shallow shells

M. Amabili*

Dipartimento di Ingegneria Industriale, Università di Parma, 43100 Parma, Italy

Abstract

Large-amplitude (geometrically non-linear) vibrations of doubly curved shallow shells with rectangular boundary, simply supported at the four edges and subjected to harmonic excitation normal to the surface are investigated. Both Donnell's and Novozhilov's shell theories are used to calculate the elastic strain energy. In-plane inertia and geometric imperfections are taken into account. The solution is obtained by Lagrangian approach. Numerical results are compared to those available in the literature and convergence of the solution is shown. Internal resonances are also studied. Shell stability under dynamic load is also investigated by using continuation method, bifurcation diagram from direct time integration and calculation of the Lyapunov exponents. Interesting phenomena, such as (i) snap-through instability, (ii) subharmonic response, (iii) period doubling bifurcations, and (iv) chaotic behavior with up to four positive Lyapunov exponents, have been observed.

Keywords: Shells; Curved panels; Double curvature; Nonlinear vibrations; Large-amplitude vibrations; Chaos; Lyapunov exponents

1. Introduction

Doubly curved panels are largely used in aeronautics and aerospace and are subjected to dynamic loads that can cause vibration amplitude of the order of the shell thickness, giving rise to significant non-linear phenomena. An exhaustive literature review of work on the non-linear vibrations of curved panels and shells is given by [1], mainly focusing on circular cylindrical shells. Pioneers in the study of large-amplitude vibrations of simply supported, circular cylindrical shallow-shells were [2] and [3]. Leissa et al. [4] studied linear and non-linear free vibrations of doubly curved shallow shells of rectangular boundaries, simply supported at the four edges without in-plane restraints. Large amplitude vibrations of shallow shells such as elliptic paraboloids, parabolic cylinders and hyperbolic paraboloids, with zero displacements and rotational springs at the four boundaries were investigated in [5–7]. Kobayashi et al. [8] studied free vibrations of doubly curved thick shallow shells. Free vibrations of doubly curved, laminated, clamped shallow shells with rectangular boundary were investigated in [9]. Soliman et al. [10] studied large amplitude, forced vibrations and stability of axi-symmetric shallow spherical shells. The approach used in the present study is discussed in [11].

2. Theoretical approach

A doubly curved shallow (small rise compared with the smallest radius of curvature) shell with rectangular boundary is considered. A curvilinear coordinate system $(O; x, y, z)$, having the origin O at one edge of the panel is assumed; $x = \psi R_x$ and $y = \theta R_y$ where ψ and θ are the angular coordinates and R_x and R_y are principal radii of curvature (constant); a and b are the curvilinear lengths of the edges and h is the shell thickness. The smallest radius of curvature at every point of the shell is larger than the greatest lengths measured along the middle surface of the shell. The displacements of an arbitrary point of coordinates (x, y) on the middle surface of the shell are denoted by u, v and w, in the x, y and z directions, respectively; w is taken positive outwards the center of the smallest radius of curvature. Initial imperfections of the shell associated with zero initial tension are denoted by out-of-plane displacement w_0, also positive outwards; only out-of-plane initial imperfections are considered.

Two different theories are used: (i) Donnell's, and (ii)

* Tel.: +39 0521 905896; Fax: +39 0521 905705; E-mail: marco@me.unipr.it

Computational Fluid and Solid Mechanics 2005
K.J. Bathe (Editor)

Novozhilov's non-linear shell theories. According to these two theories, the strain components ϵ_x, ϵ_y and γ_{xy} at an arbitrary point of the panel are related to the middle surface strains $\epsilon_{x,0}$, $\epsilon_{y,0}$ and $\gamma_{x,y,0}$ and to the changes in the curvature and torsion of the middle surface k_x, k_y and k_{xy} by the following three relationships:

$$\varepsilon_x = \varepsilon_{x,0} + z\,k_x, \quad \varepsilon_y = \varepsilon_{y,0} + z\,k_y, \quad \gamma_{xy} = \gamma_{xy,0} + z\,k_{xy}, \tag{1}$$

where z is the distance of the arbitrary point of the panel from the middle surface. The middle surface strain–displacement relationships and changes in the curvature and torsion have different expressions for the Donnell's and Novozhilov's theories not reported here.

The elastic strain energy U_S of the shell, neglecting σ_z as stated by Love's first approximation assumptions, is given by

$$U_S = \frac{1}{2}\int_0^a\int_0^b\int_{-h/2}^{h/2} \left(\sigma_x\,\varepsilon_x + \sigma_y\,\varepsilon_y + \tau_{xy}\,\gamma_{xy}\right) (1 + z/R_x)\,(1 + z/R_y)\mathrm{d}x\,\mathrm{d}y\,\mathrm{d}z, \tag{2}$$

where the stresses σ_x, σ_y and τ_{xy} are related to the strain for homogeneous and isotropic material by simple expressions for plane stress.

The kinetic energy T_S of the shell, by neglecting rotary inertia, is given by

$$T_S = \frac{1}{2}\rho_S\,h\int_0^a\int_0^b (\dot{u}^2 + \dot{v}^2 + \dot{w}^2)\,\mathrm{d}x\,\mathrm{d}y \tag{3}$$

where ρ_S is the mass density of the shell.

The nonconservative damping forces are assumed to be of viscous type and are taken into account by using the Rayleigh's dissipation function

$$F = \frac{1}{2}c\int_0^a\int_0^b \left(\dot{u}^2 + \dot{v}^2 + \dot{w}^2\right)\mathrm{d}x\,\mathrm{d}y \tag{4}$$

where c has a different value for each term of the mode expansion.

The virtual work W done by the external forces is written as

$$W = \int_0^a\int_0^b \left(q_x\,u + q_y\,v + q_z w\right)\mathrm{d}x\,\mathrm{d}y \tag{5}$$

where q_x, q_y and q_z are the distributed forces per unit area acting in x, y and normal directions, respectively.

The generalized forces Q_j are obtained by differentiation of the Rayleigh's dissipation function and of the virtual work done by external forces:

$$Q_j = -\frac{\partial F}{\partial \dot{q}_j} + \frac{\partial W}{\partial q_j} \tag{6}$$

The Lagrange equations of motion are

$$\frac{\mathrm{d}}{\mathrm{d}t}\left(\frac{\partial T_S}{\partial \dot{q}_j}\right) - \frac{\partial T_S}{\partial q_j} + \frac{\partial U_S}{\partial q_j} = Q_j, \quad j = 1, \ldots dof \tag{7}$$

where $\partial T_s/\partial q_j = 0$. The very complicated term giving quadratic and cubic non-linearities can be written in the form

$$\frac{\partial U_S}{\partial q_j} = \sum_{k=1}^{dofs} q_k \tilde{z}_{j,k} + \sum_{i,k=1}^{dofs} q_i\,q_k \tilde{z}_{j,i,k} + \sum_{i,k,l=1}^{dofs} q_i\,q_k\,q_l\,\tilde{z}_{j,i,k,l} \tag{8}$$

where coefficients $\tilde{z}$ have long expressions that include also geometric imperfections.

3. Numerical results

Numerical calculations have been initially performed for doubly curved shallow shells, simply supported at the four edges, having the following dimensions and material properties: curvilinear dimensions $a = b = 0.1$ m, radius of curvature $R_x = 1$ m, thickness $h = 0.001$ m, Young's modulus $E = 206 \times 10^9$ Pa, mass density $\rho = 7800\,\mathrm{kg/m^3}$ and Poisson ratio $\nu = 0.3$. Shallow shells with the same dimension ratios ($R_x/a = 10$, $h/a = 0.01$, $a/b = 1$, $\nu = 0.3$) were previously studied by [8]. In all the numerical simulations a modal damping $\zeta_{1,1} = 0.004$ and harmonic force excitation at the center of the shell in z direction are assumed. If not explicitly specified, all calculations have been performed by using Donnell's shell theory. A spherical shallow shell ($R_x/R_y = 1$, $R_y = 1$ m) is initially considered. The frequency range around the fundamental frequency (mode ($m = 1$, $n = 1$) in this case, where m and n are the numbers of half-waves in x and y direction, respectively) is investigated. The fundamental frequency $\omega_{1,1}$ is 952.31 Hz, according with Donnell's shell theory. The amplitude of the harmonic force is $\tilde{f} = 31.2$ N. Comparison of the response computed with the 22 and 9 degrees of freedom (*dof*) models is given in Fig. 1, where the backbone curve of [8] is also shown. The results of the 22 *dof* model are moved slightly to the left with respect to the smaller 9 *dof* model, and present a more complex curve, specially in the frequency region around $0.9\omega_{1,1}$. In fact, for excitation frequency, $\omega = 0.9\,\omega_{1,1}$, there is a 3:1 internal resonance with modes ($m = 3$, $n = 1$) and ($m = 1$, $n = 3$), giving $3\omega = \omega_{3,1} = \omega_{1,3}$. A

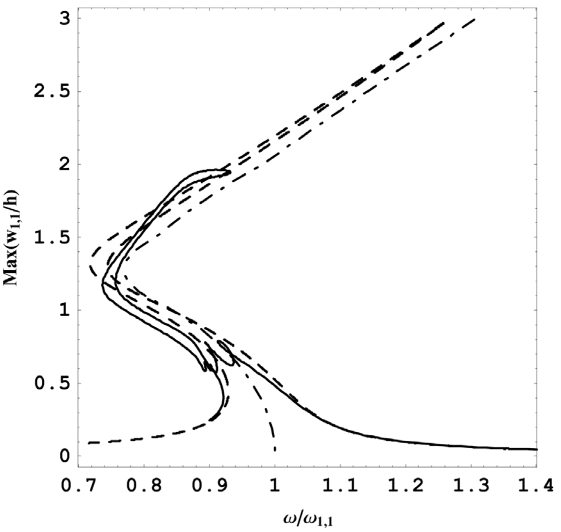

Fig. 1. Amplitude of the response of the shell *versus* the excitation frequency; $R_x/R_y = 1$ (spherical shell); fundamental mode ($m = 1, n = 1$), $\tilde{f} = 31.2$ N and $\zeta_{1,1} = 0.004$; Donnell's theory. Thick rule represents 22 *dof* model; broken rule represents 9 *dof* model backbone curve from [8].

second relationship between natural frequencies that leads to internal resonances is for $\omega = 0.77\ \omega_{1,1}$ where $6\omega = \omega_{3,3}$.

Figure 2 synthesizes all the maximum responses for the 9 *dofs* model for different shell curvature aspect

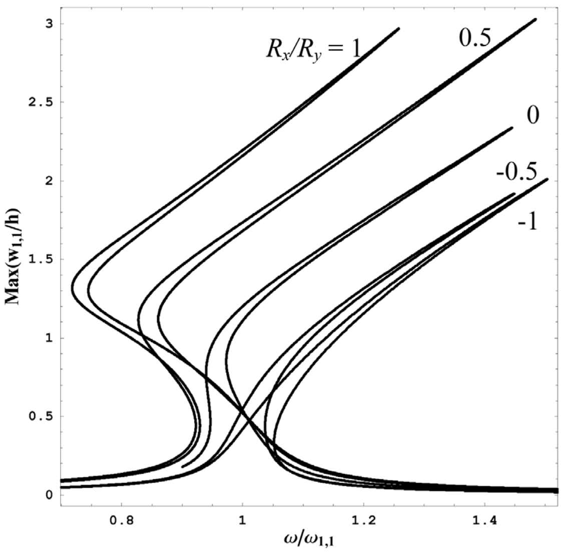

Fig. 2. Effect of the curvature aspect ratio R_x/R_y on the shell response (maximum of the generalized coordinate $w_{1,1}$) *versus* the excitation frequency; fundamental mode ($m = 1, n = 1$); $\zeta_{1,1} = 0.004$; 9 *dof* model; Donnell's theory.

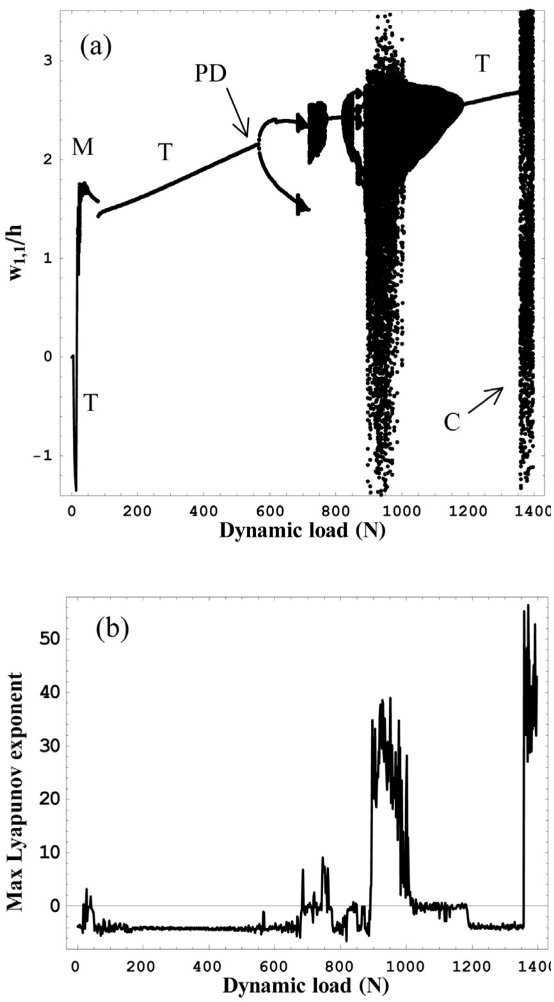

Fig. 3. Bifurcation diagram of Poincaré maps and maximum Lyapunov exponent for the spherical shallow shell under decreasing harmonic load with frequency; $\omega = 0.8\omega_{1,1}$; $\zeta_{1,1} = 0.004$; 22 *dof* model; Donnell's theory. (a) Bifurcation diagram: generalized coordinate $w_{1,1}$; T = response period equal to excitation period; PD = period doubling bifurcation; M = amplitude modulations; C = chaos; (b) maximum Lyapunov exponent.

ratios R_x/R_y. It is clearly shown that for $R_x/R_y = 1$ (spherical), 0.5 and 0 (circular cylindrical) the shallow shell considered exhibits a softening type behaviour turning to hardening type for vibration amplitude of the order of magnitude of the shell thickness. The softening behaviour becomes weaker with the decrement of the curvature aspect ratio R_x/R_y.

The same shallow spherical shell studied in Fig. 1 is considered again and the 22 *dof* model is used. Poincaré maps have been computed by direct integration of the

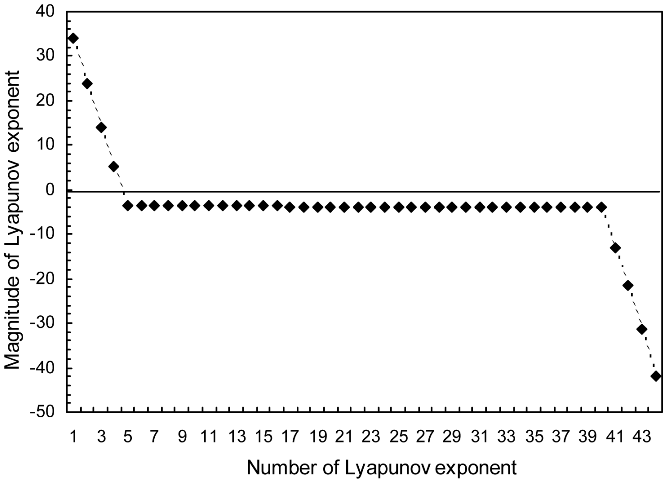

Fig. 4. All 44 Lyapunov exponents for the spherical shallow shell; excitation frequency $\omega = 0.8\omega_{1,1}$, $\tilde{f} = 1396\,\mathrm{N}$ and $\zeta_{1,1} = 0.004$; 22 *dof*.

equations of motion. The excitation frequency has been kept constant, $\omega = 0.8\omega_{1,1}$. The bifurcation diagrams obtained by all these Poincaré maps are shown in Fig. 3, where the load is decreased from 1400 N to 0. Simple periodic motion, period doubling bifurcation, subharmonic response, amplitude modulations and chaotic response have been detected, as indicated in Fig. 3. This indicates a very rich and complex nonlinear dynamics of the spherical shallow shell subject to large harmonic excitation. Different stable solutions coexist for the same set of system parameters, so that the solution is largely affected by initial conditions. In particular, Fig. 3(b) gives the maximum Lyapunov exponent σ_1 associated with the bifurcation diagram. It can be easily observed that (i) for periodic forced vibrations $\sigma_1 < 0$, (ii) for amplitude modulated response $\sigma_1 = 0$, and (iii) for chaotic response $\sigma_1 > 0$. Therefore σ_1 can be conveniently used for identification of the system dynamics. All the Lyapunov exponents have been evaluated for the case with excitation $\tilde{\mathrm{f}} = 1396$ N corresponding to chaotic response, see Fig. 4. In this case, four positive Lyapunov exponents have been identified, allowing to classify this response as hyperchaos. The Lyapunov dimension in this case is $d_L = 24.59$.

Acknowledgements

This work was partially supported by the FIRB 2001 and COFIN 2003 grants of the Italian Ministry (MIUR).

References

[1] Amabili M, Païdoussis MP. Review of studies on geometrically nonlinear vibrations and dynamics of circular cylindrical shells and panels, with and without fluid-structure interaction. Appl Mech Rev 2003;56:349–381.
[2] Reissner E. Nonlinear effects in vibrations of cylindrical shells. Ramo-Wooldridge Corporation Report AM5–6, 1955.
[3] Grigolyuk EI. Vibrations of circular cylindrical panels subjected to finite deflections (in Russian). Prikladnaya Matematika i Mekhanika 1955;19:376–382.
[4] Leissa AW, Kadi AS. Curvature effects on shallow shell vibrations. J Sound Vib 1971;16:173–187.
[5] Bhattacharya AP. Nonlinear flexural vibrations of thin shallow translational shells. ASME J Appl Mech 1976;43:180–181.
[6] Sinharay GC, Banerjee B. Large-amplitude free vibrations of shallow spherical shell and cylindrical shell – a new approach. Int J Non-Linear Mech 1985;20:69–78.
[7] Sinharay GC, Banerjee B. Large-amplitude free vibrations of shells of variable thickness – a new approach. AIAA J 1986;24:998–1004.
[8] Kobayashi Y, Leissa AW. Large amplitude free vibration of thick shallow shells supported by shear diaphragms. Int J Non-Linear Mech 1995;30:57–66.
[9] Abe A, Kobayashi Y, Yamada G. Non-linear vibration characteristics of clamped laminated shallow shells. J Sound Vib 2000;234:405–426.
[10] Soliman MS, Gonçalves PB. Chaotic behaviour resulting in transient and steady state instabilities of pressure-loaded shallow spherical shells. J Sound Vib 2003;259:497–512.
[11] Amabili M. Comparison of shell theories for large-amplitude vibrations of circular cylindrical shells: Lagrangian approach. J Sound Vib 2003;264:1091–1125.